3D porous media reconstruction from 2D slices with deep learning models

Alexey Olkhovikov Maksimilian Pavlov Aziz Temirkhanov Gleb Komissarov

Abstract

In petroleum engineering especially during reservoir exploration and simulation it is needed to know the structure of pores to obtain an accurate multi phase flow model. In our paper we propose a method of three-dimensional media reconstruction by using deep neural networks: generative adversarial networks (GAN) and denoising diffusion probabilistic models (DDPM). Based on the lowest slices of 3D image we were able to obtain the three-dimensional structure around such slices as the most probable one according to that constructed distribution.

Github repository: link
Video presentation: link

1. Introduction

In order to obtain 3D image of rock sample there is widely used type of microscopes called SEM (scanning electron microscope).It is a type of electron microscope that produces images of a sample by scanning the surface with a focused beam of electrons. The electrons interact with atoms in the sample, producing various signals that contain information about the surface topography and composition of the sample (Stokes, 2008). FIB-SEM microscope is an essential part of digital rock technology which is highly important in reservoir simulation. The technology aims at the calculation of various physical properties of a rock sample based on its digital representation. The list of properties can include storage properties such as porosity, open porosity, connected porosity, and fractional porosity; transport properties such as permeability, relative phase permeability, and capillary pressure; electromagnetic properties such as the formation factor, dielectric permittivity, and magnetic and electric permeabilities; elastic coefficients; geomechanical constants; and characteristics of NMR response and responses to other good logging signals (N. Evseev & Safonov, 2015)

3D imaging is conducting during focused ion beaming which is really long-lasting and costly procedure. Obstacles blocking wider adoption of FIB-SEM include slow imaging speed and lack of long-term system stability, which caps the maximum possible acquisition volume. And sometimes 3D FIB-SEM can not be used due to the specific properties of rock sample and, moreover, not all core sample are accessible due to their loss. Thus, generating 3D micro-structure from 2D images is a really useful tool because it can save time and money. We propose to apply deep learning models to model three-dimensional textures of rocks based on three-dimensional binary representations of porous media acquired at the micrometer scale.

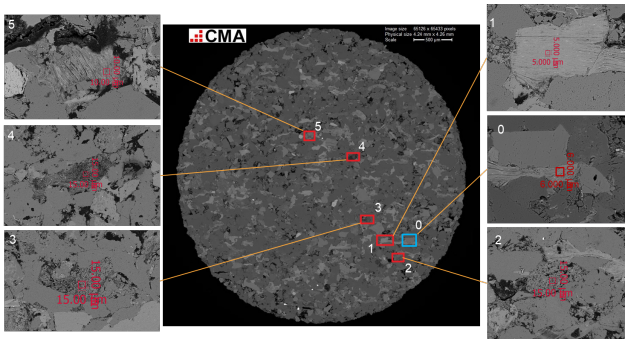

Figure 1. SEM imaging

Generative Adversarial Networks (GAN) (Ian J. Goodfellow, 2014) have generated realistic images with diversity, however the majority of these approaches are based on 2D image generation. Due to the high-memory requirements of GANs, large networks cannot easily be applied directly for high quality 3D image synthesis. Recently, DDPMs (Ho et al., 2020) have emerged as a powerful family of generative models without adversarial training, showing superior performance and being widely studied in various image processing tasks. In this paper, we present 3D DDPM and 3D GAN to enable high quality three dimensional images of porous media and compared our proposed model to them.

2. Related work

In their work (Lukas Mosser & Blunt, 2017) developed volumetric version of DCGAN network. The network consists of two independent fully convolutional neural networks, the generator G and the discriminator D. Upsampling from the input latent vector z is performed by volumetric transposed convolution, followed by batch normalization and a rectified linear unit (ReLU) activation function in all lay-

ers except the last. The discriminator D receives images sampled from the latent space by the generator G(z) and images from the set of training images representing pdata(x). Therefore, the size of the input layer of the discriminator corresponds to the dimensions of the input training images. The discriminator consists of volumetric convolution layers combined with LeakyReLU activation functions [46]. The final convolutional layer of the discriminator is followed by a sigmoid activation function. Images generated by the GAN were post-processed using a 33 median filter to remove single-pixel noise. The final GAN models were subsequently evaluated in terms of their directional and radial averaged noncentered covariance S2(r), Minkowski functionals and the single-phase permeability. The work proved that the synthetic images generated by the GAN model are able to capture the characteristic statistical and physical behavior of these porous media. One of the disadvantages which may be pointed out in their work is that they don't parameterize noise what can be worsen the output of a model.

Reference of (Volkhonskiy D., 2022) provides a working framework of 3D media reconstruction using GAN based deep learning architecture. They used custom architecture called slice pore generative adversarial network (SPGAN) which is a synergy of a convolutional autoencoder and 3D deep convolutional generative adversarial network. It can be considered as a deep convolutional generative adversarial network, where the generator is conditioned on the noise and the latent representation of the 2D slice (fig. 2).

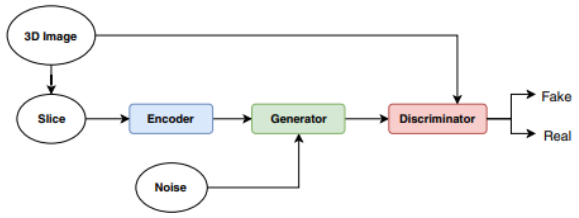

Figure 2. Architecture of slice to pores generative adversarial networks (Volkhonskiy D., 2022)

Autoencoder takes 2D central slice images from 3D image which is obtained by loss function (1):

$$L(s) = ||s - M \odot G_\theta(E_\tau(s), z)||_2^2 \rightarrow min_{\tau,\theta} \quad (1)$$

This loss function provide a minimization between the input slice s and the central slice M $\odot$ (E (s),z) in the generated 3D image. Therefore, generator take as an input 2D lowest slice and noise. Two estimate the quality of algorithm authors compared permeability, porosity, two-point correlation and so-called Minkowski functionals for a set of real and a set of generated samples.

In paper by (Dorjsembe Z., 2022) authors implemented DDPM model to to enable 3D medical image synthesis. Deep learning was used for generating high-resolution magnetic resonance images (MRI) of brain tumor. The architecture is presented on figure 3. Moreover, DDPM was compared with CCE-GAN, 3D-alpha-GAN by Multi-Scale Structural Similarity (MS-SSIM), which measures the diversity of generated images. DDPM demonstrated better results than GAN's models.

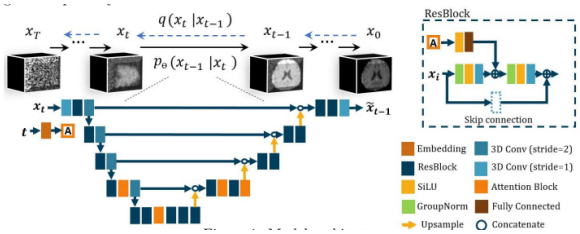

Figure 3. DDPM architecture

3. Algorithms and Models

3.1. Deep convolution generative adversarial networks (DCGAN)

We were inspired by architecture of (Volkhonskiy D., 2022) and tried to build similar DCGAN in our own style. The architecture of DCGAN generator is presented on figure 4.

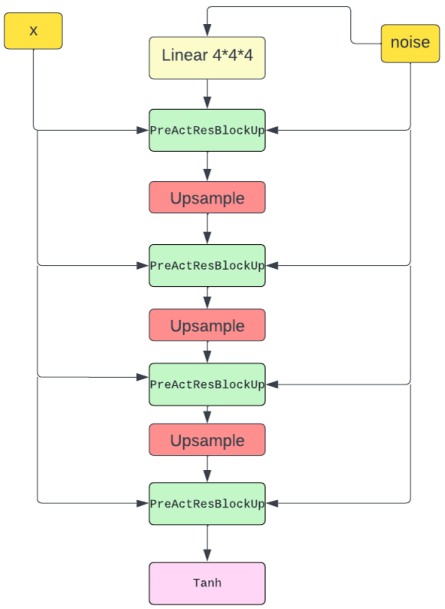

Figure 4. DCGAN generator

The main idea of generator architecture is that every input of residual block parameterize with noise and embed-

dings which were obtained from encoder. Encoder extracts the lowest slice from 3D image and passes to the input of generator. Architecture of encoder was implemented as in EfficientNet (b3 version) by (Mingxing Tan, 2019). Discriminator has standard downstream architecture (fig. 5).

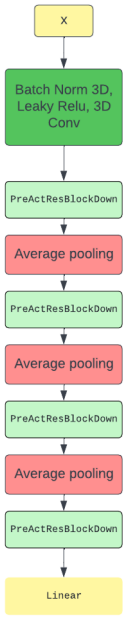

Figure 5. DCGAN discriminator

For generator we used mean squared error loss function (eq. 1). For discriminator we tried binary cross-entropy loss with logits and Wasserstein loss.

Binary cross-entropy loss:

$$BCE(s) = -w_n[y_n \cdot log\sigma(x_n) + (1-y_n) \cdot log(1-\sigma(x_n))] \quad (2)$$

Wasserstein loss:

$$L(s) = D(x) - D(G(z)) \quad (3)$$

3.2. Denoising diffusion probabilistic model (DDPM)

Diffusion deep neural network is based on UNet architecture (fig. 6). Standard Adam optimizer with default hyperparameters was used for training. Also, L1 loss was chosen as main for training the model:

$$L1 = |y_{true} - y_{pred}| \quad (4)$$

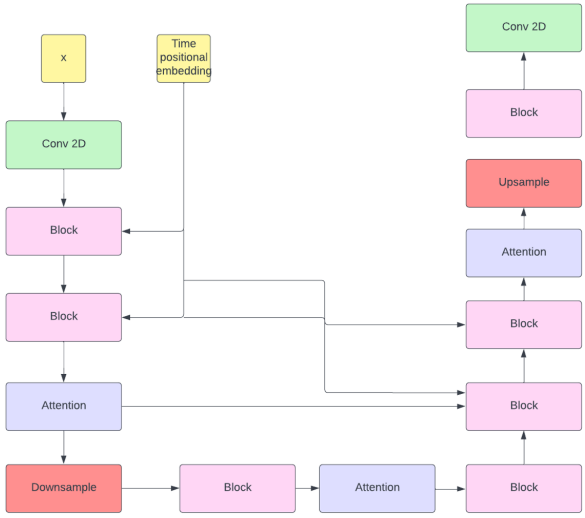

Figure 6. Architecture of DDPM UNet

4. Experiments and results

Except DCGAN and DDPM deep learning models BIGGAN (Brock A., 2019) model was trained. However, this model requires non-local block which is a close to the meaning to self-attention block and in 3D case takes high computational power. Because of that non-local block was excluded and result of training BIGGAN without non-local block was poor. All training data was augmented by geometrical augmentations (random horizontal flip, random rotation, random vertical flip). Unfortunately, more augmentations highly change the morphology of train dataset, thus, it is needed more epochs and more computational power which is limited especially in 3D images generation case.

To evaluate the quality of synthetic data, we compared porosity, and Minkowski functionals for a set of real and a set of generated samples. Also visual analysis of generated sample and real sample was conducted in order to validate the quality of deep learning networks. Before applying evaluating algorithm to calculate porosity, conduct permeability calculations in future research, all test set was binarized by using OpenCV library.

4.1. DCGAN results

Model was trained for 4500 epochs and batch size of 4 3D cubes per 1 GPU (3 GPU's in total). Looking at 2D slices of 3D cubes (appendix, fig. 10,11) we found that DCGAN had problem with generating pore structure on the border of a cube (fig. 12) while the central part was generated with quite similar structure. Porosity and Minkowski functionals demonstrate that obtained by DCGAN distributions are pretty close to initial one, thus, DCGAN could reconstruct

the pore structure in some extent.

4.2. DDPM results

Firstly, we built 3D DDPM neural network it was significantly difficult to train this model because it is needed to perform more than several thousands epochs which our equipment doesn't allow to perform. Therefore, we decided to build 2D DDPM model for slices generation. We tried several noise time steps (1000, 500, 100) and stopped at 100 time steps. Unfortunately, through the 1000 of epoch we couldn't obtain good results (fig. 16). Results were too noisy and there is no any sign of the network to learn any patterns of the images. The main reason why it is happened in our opinion is that initial inputs even denoised contained some kind of noise and didn't have obvious patterns to learn in 2D case.

5. Conclusion

In our work we trained three generative models: modified DCGAN with several inputs, BIGGAN and denoising diffusion probabilistic model (DDPM). The best results were obtained by modified DCGAN which porosity, minkowski functionals were close to the initial distribution of 3D cubes. 3D BIGGAN with non-local block were impossible to train on our training equipment, it needs much more computational power to train neural network with 3D self-attention block. BIGGAN without non-local block couldn't achieve comparable results. In DDPM case we trained our 2D model for 1000 epoch and still got a random noise instead of images. Therefore, this type of models should be examined further for the given task.

References

Brock A., Donahuet J., S. K. Large scale GAN training for high fidelity natural image synthesis. *ICLR conference*, 2019.

Dorjsembe Z., Odonchimed S., X. F. Three-dimensional medical image synthesis with denoising diffusion probabilistic models. *MIDL*, 2022. doi: 10.1016/j.jcp.2018.10.001.

Ho, J., Jain, A., and Abbeel, P. Denoising diffusion probabilistic models. *arXiv preprint arxiv:2006.11239*, 2020.

Ian J. Goodfellow, j Pouget-Abadie, M. M. B. X. Generative adversarial networks. *Cornel university*, 2014.

Lukas Mosser, Olivier Dubrule, nd Blunt, M. J. Reconstruction of three-dimensional porous media using generative adversarial neural networks. *Physical review*, 2017. doi: https://doi.org/10.1103/PhysRevE.96.043309.

Mingxing Tan, Q. V. L. Efficientnet: Rethinking model scaling for convolutional neural networks. *International Conference on Machine Learning*, 2019.

N. Evseev, O. Dinariev, M. H. and Safonov, S. Coupling multiphase hydrodynamic and NMR pore-scale modeling for advanced characterization of saturated rocks. *Petrophysics*, 2015.

Stokes, D. J. Principles and practice of variable pressure environmental scanning electron microscopy (vp-esem). *John Wiley Sonse*, 2008. ISSN ISBN 978-0470758748.

Volkhonskiy D., Muravleva E, S. O. O. D. B. E. K. D. Generative adversarial networks for reconstruction of three-dimensional porous media from two-dimensional slices. *Physical review*, 2022.

A. Team member's contributions

Explicitly stated contributions of each team member to the final project.

Alexey Olkhovikov

- Data preprocessing.
- DCGAN implemetation, training and testing.
- Loss finctions implementation.
- 2D Denoising Diffusion Probabilistic model adoptation for a given task (Dataloader), training and testing.
- Denoising Diffusion Probabilistic model adoptation for a 3D case, training and testing.
- Partially implemented BIGGAN (Generator).

Maksimilian Pavlov

- Metrics calculations and comparisons.
- Partially implemented BIGGAN (non-local block and discriminator) architecture, training and testing.
- Different encoders testing.
- Report and presentation preparation.
- Video preparation.

Aziz Temirkhanov

- 1 commit into repository without any results.

Gleb Komissarov

- Participated in two calls.

B. Third party code list

DDPM model: link

EfficientNet-b3 model: link

C. Appendix

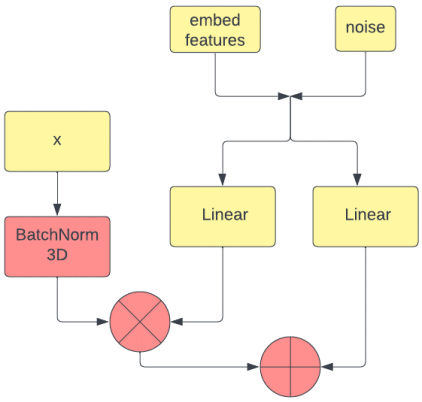

Figure 7. Adaptive batch norm

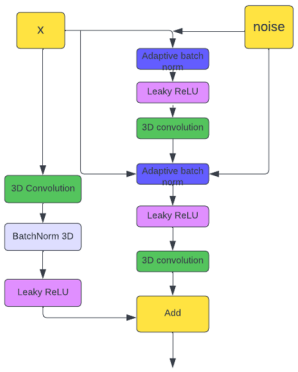

Figure 8. Preactivated residual block in generator of DCGAN

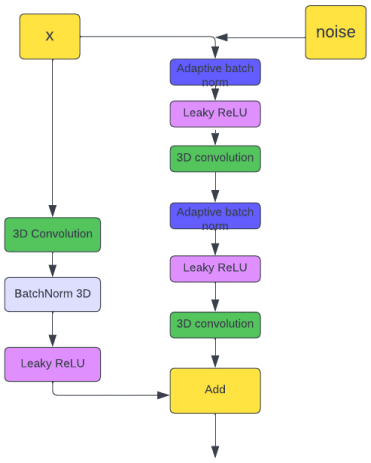

Figure 9. Preactivated residual block in discriminator of DCGAN

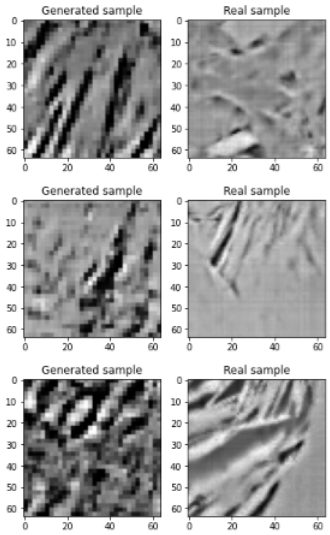

Figure 10. DCGAN results on central 2D sliced of test cubes before denoising

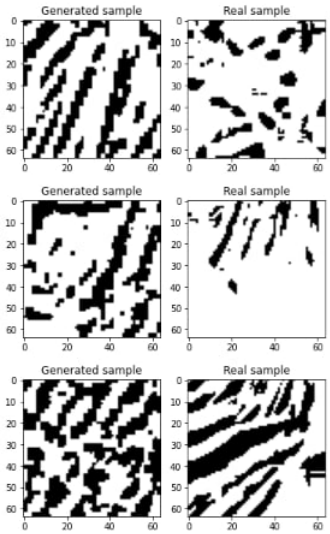

Figure 11. DCGAN results on central 2D sliced of test cubes after denoising

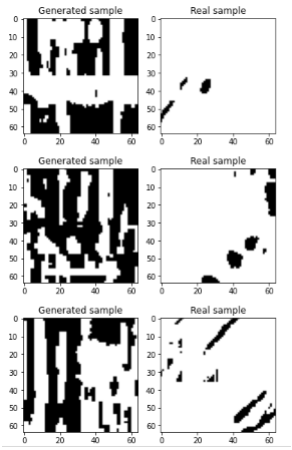

Figure 12. Unpleasant results DCGAN at the edge of a cube

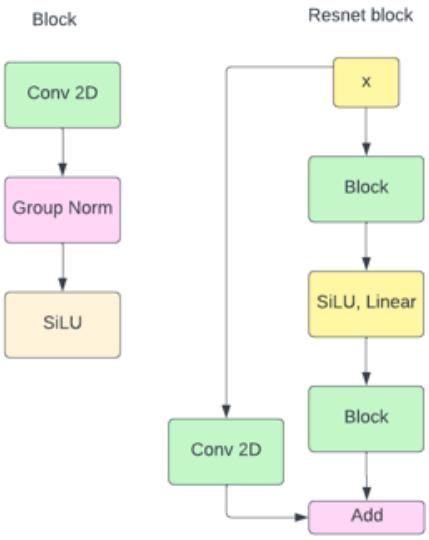

Figure 15. Diffusion block of DDPM neural network

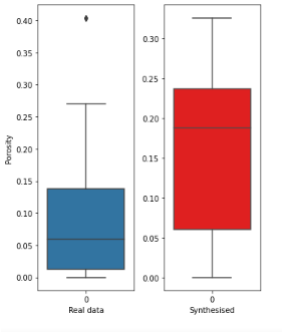

Figure 13. Porosity distribution of test and generated samples

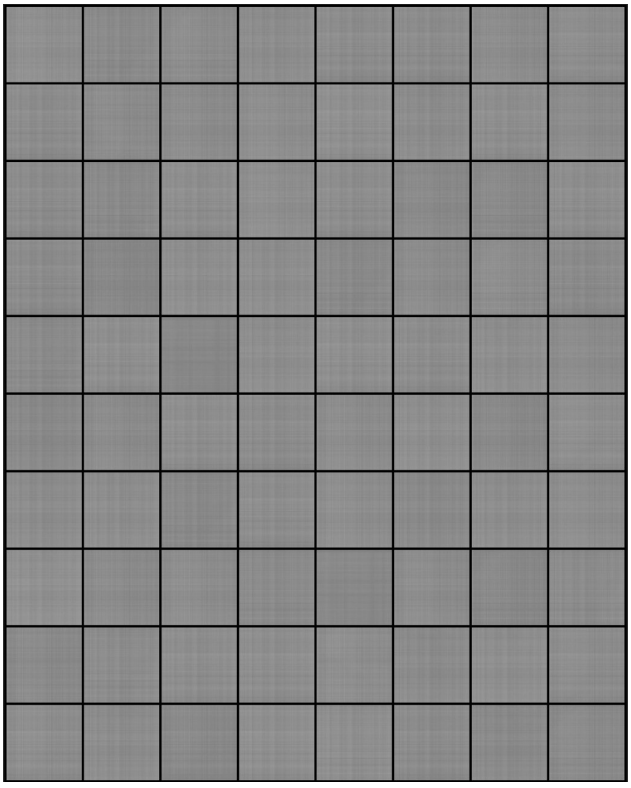

Figure 16. Results of 1000 epoch of DDPM training

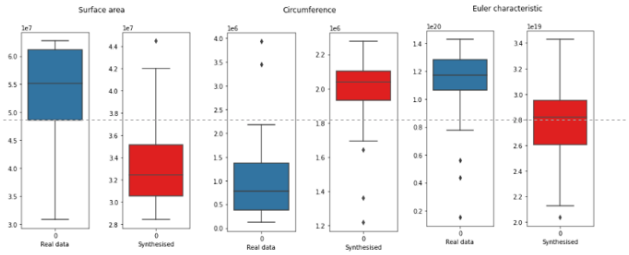

Figure 14. Minkowski characteristic for test data and DCGAN generated samples